

---

## Optimal region growing and multi-kernel SVM for fault detection in electrical equipments using infrared thermography images

---

C. Shanmugam\*

Jansons Institute of Technology,  
Coimbatore, India  
Email: cshanmugamphd@gmail.com  
Email: erodeshanmugam@gmail.com  
\*Corresponding author

E. Chandira Sekaran

Coimbatore Institute of Technology,  
Coimbatore, India  
Email: chandirasekarane07@gmail.com  
Email: ecseecit@gmail.com

**Abstract:** Infrared thermography (IRT) has played an essential part in observing and examining thermal defects of electrical equipment without ending, which has vital enormity for the dependability of electrical recorded. This paper dissected the electrical parts are faulted or non-faulted with the help of segmentation and classification model. The features are calculated from the input thermal images and regions of interest (ROI) is segmented by utilising optimal region growing (ORG) technique and faults are classified using multi kernel support vector machine (MKSVM). In the tests, the classification performances from different input features are assessed. For enhancing the performance of the segmentation investigation optimisation procedure that is whole optimisation (WO) is used. Before classifying, the extracted electrical components are fused by using feature level fusion (FLF) procedure to fused vector in all images. These multi kernel classification performance indices, including sensitivity, specificity and accuracy are utilised to recognise the most appropriate input feature and the best arrangement of classifiers. The performance of SVM is contrasted with a neural network. The correlation comes about demonstrating that our technique can accomplish a superior performance with accuracy at 98.21%.

**Keywords:** infrared thermography; IRT; feature extraction; support vector machine; SVM; optimisation; classification and fault detection.

**Reference** to this paper should be made as follows: Shanmugam, C. and Sekaran, E.C. (2020) 'Optimal region growing and multi-kernel SVM for fault detection in electrical equipments using infrared thermography images', *Int. J. Business Intelligence and Data Mining*, Vol. 17, No. 3, pp.329–348.

**Biographical notes:** C. Shanmugam received his BE in Electrical and Electronics Engineering from the Institute of Road and Transport Technology, Erode and ME in Applied Electronics from the Coimbatore Institute of Technology. He is currently working as an Assistant Professor in the Department of Electronics and Communication Engineering, Jansons Institute

of Technology, Coimbatore, Tamil Nadu, India. He has two years of industrial and 13 years in teaching experience. He has published six research papers in national/international journals and national/international conferences. He received research funds from HRD, NBHM (DAE). His research interests are in electrical system analysis, image processing and soft computing.

E. Chandira Sekaran received his BE in Electrical and Electronics Engineering from PSG College of Technology and ME in Applied Electronics from the Coimbatore Institute of Technology. He obtained his PhD in Electrical Engineering from the Anna University-Chennai. He is currently working as a Professor in the Department of Electrical and Electronics Engineering, Coimbatore Institute of Technology, Coimbatore, Tamil Nadu, India. He has two years of industrial and 25 years in teaching experience. He has published 57 research papers in national/international journals and national/international conferences. He is the Principal Investigator in the research projects of CPRI, CDAC, DST, AICTE and UGC. His research interests are in power electronics, power quality, renewable energy sources, energy conservation and management.

---

## 1 Introduction

The maintenance of electrical instrumentation is often a challenge for the ability business attributable to the massive range of electrical instrumentation and also the shortage of personnel. The repair and maintenance of a facility are often classified beneath three different categories:

- 1 instrumentation malfunction
- 2 time-based deterioration in performance attributable to aging, poor maintenance, etc.
- 3 condition-based maintenance (CBM).

The most widespread one is CBM, conjointly referred to as preventive maintenance. CBM was introduced to do and maintain the right instrumentality at the correct time. CBM relies on exploitation period of time knowledge to the range and optimises maintenance resources. Perceptive the state of the system is understood as condition observation. Such a system can confirm the equipment's health and act only if maintenance is truly necessary. Ideally, condition-based monitoring can enable the upkeep personnel to try to solely the correct things, minimising spare components price, system period of time and time spent on maintenance.

A major cause for failure in electrical equipment is the effect of heating due to circuit malfunction. Abnormalities within the instrumentality can occur once their internal temperatures exceed their limits. Consequently, the warming of electrical instrumentality will result in subsequent failure of the instrumentality and may doubtless end in unplanned outages, injury and health hazard. The common issues concerning thermal anomalies in electrical installations are loose or poor connections, unbalanced loads, short circuits, overloading and cracks or defects within the instrumentality body (Ahmed et al., 2015).

Infrared thermography (IRT) is well known as one of the effective tools for monitoring the condition of equipment. It uses infrared sensors and optical lenses in a

constructed electrical circuitry to capture images of thermal objects based on temperature variations. Infrared thermal camera stores the infrared pictures of thermal objects as thermal images that the human can see in order to understand the inside conditions of the objects. With the images, inspectors can analyse the temperature variations of thermal objects to look for defective parts. Also, the effective maintenance of equipment in most cases would require the presence of well experienced and trained personnel in order to analyse the infrared images and perform an accurate prognosis. However, this might not be an optimum solution due to a shortage of staff (Sujatha and Shalini Punithavathani, 2018; Sundararaj, 2016). Hence, by feeding the images to an intelligent system, an accurate diagnosis can be obtained and read even in the absence of experts (Jadin et al., 2014).

In this paper, fault diagnosis using optimal region growing (ORG) and multi kernel support vector machine (MK SVM) on thermography images. The input images are firstly pre-processed and then the ROI is segmented using ORG algorithm. In ORG method, whale optimisation (WO) is used to find the suitable threshold selection and to improve the segmentation process. Once segmentation is completed, the fault diagnosis is performed using MK SVM.

The main contributions of this paper are summarised as follows:

- We present a WO based threshold selection algorithm is proposed to improve the standard region growing (RG) algorithm.
- We design a MK SVM method to classify the fault in thermography images. Here, linear and quadratic kernels are used.
- We perform extensive simulation on the proposed algorithm, compare and analyse results with existing and related algorithms.

The paper is organised as follows. The related work is discussed in Section 2. The proposed fault diagnosis approach is described in Section 3. The experimental result is explained in Section 4. Finally, the paper is concluded in Section 5.

## **2 Review of related works**

In recent years, a variety of approaches have been presented for fault diagnosis on thermography images. In Stoicescu et al. (2014), daylight luminescence system testing is proposed to detect the cracks in solar panels, but the drawback of this method is that it may not be suitable to detect the faults which have not occurred due to any physical damage like crack. In Tsanakas et al. (2015a), Canny edge detection is proposed to process the thermal images. The work is good but an automatic diagnosis method along with proposed canny edge detection method would have been a better supplement. In Tsanakas et al. (2015b), aerial orthophoto thermal mapping is used for fault detection in large-scale PV plants. In Chouder and Silvestre (2010), an automatic supervision and fault detection system based on power loss comparison between faulty and healthy panel is proposed. In Takashima et al. (2009), two experimental methods using Earth capacitance measurement (ECM) method and time-domain reflectometry (TDR) were studied to find the fault location in PV module strings, but the methods are too tedious as compared to IRT technique suggested in present work.

Intelligent system for fault detection in PV modules has been proposed using fuzzy logic, neuro-fuzzy network. In Riley and Johnson (2012), faults in PV panels have been detected based on a deviation in actual AC power with that of the predicted AC power by ANN. In Ducange et al. (2011), an automatic fault detection system in PV modules is proposed based on the fuzzy rule-based system, which provides a comparison between the power of a faulty and healthy system. In Coleman and Zalewski (2011), a data acquisition system for the solar power plant is presented and a list of possible fault is given. Huda et al. (2012) proposed a semi-automatic system for thermographic inspection of electrical installation within buildings. The ROI of images were manually segmented and then statistical features were extracted which were the first order histogram, the grey level co-occurrence matrix features and the differences between hot and reference regions. Principle component analysis (PCA) was used to select the best features. Finally, 15 statistical features were used as input data for a multi-layer perception (MPL) network to classify thermal conditions as normal, warning and critical. In Haddadnia and Seryasat (2010), Zernike moments were used as image features and a support vector machine (SVM) was adopted as a classifier to recognise two types of faults, i.e., the fault in the fuses cable lug and the fault in the top and bottom fuse bases. An intelligent thermal imaging diagnosis system was proposed by Almeida et al. (2009) for diagnosing faults in surge arresters. The system used watershed segmentation algorithm to find the region of interest and a neuro-fuzzy network to classify the thermal conditions into three classes as faulty, normal and suspicious. This system was validated using 100 thermal images and the validation error was about 10%. In another study (Huda et al., 2014), six features from images were selected from 15 features as a multilayered perceptron network input data and achieved 79.4% accuracy. Jaffery and Dubey (2014) developed a real-time and off-line system to monitor the temperature variations and analyse hot regions in electrical assets using IRT. In Ahmed et al. (2015), a recursively constructed output-context fuzzy system was proposed to characterise the condition of electrical hotspots. Moreover, a numerous fuzzy based classifiers have been developed in recent years (Pratama et al., 2018a, 2018b, 2016, 2015).

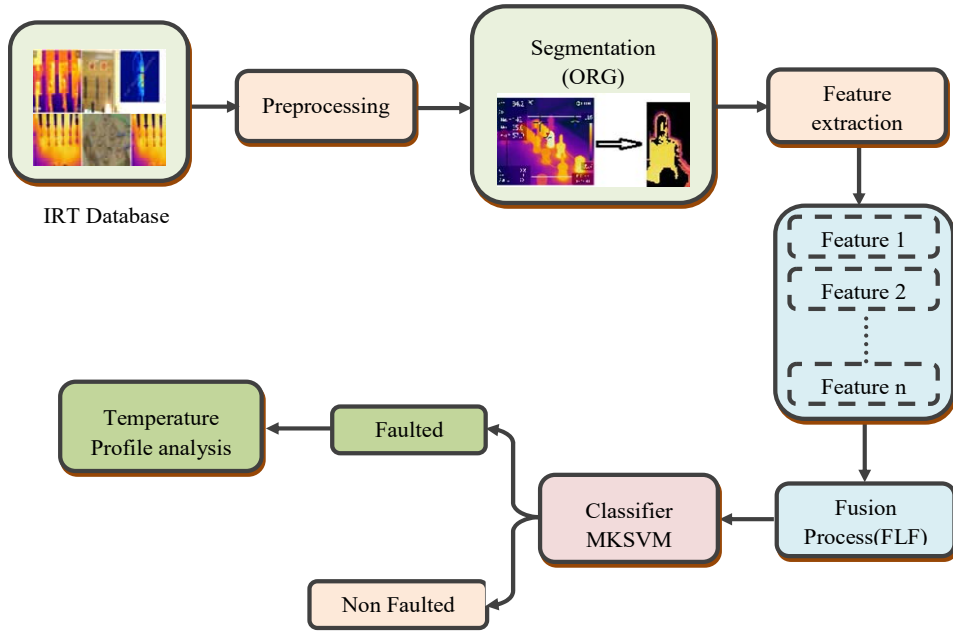
### **3 Proposed fault diagnosis system**

IRT is a thermal investigation apparatus that has been utilised for deterrent support for mechanical and electrical frameworks. The methodology mainly aims to find the faults in the electrical equipment utilising thermographic and image processing procedure. The majority IRT camera can give data about least, greatest, spot temperature and hot temperature point of an infrared image. These qualities are extremely valuable and will be utilised for promoting examination. This examination strategy comprises of four unique modules to classify fault or non-fault equipment. Primarily, the images are fed to histogram equalisation process at that point segment the constituent parts by the assistance of ORG. From the segmentation part separate the meaning full data that feature using colour and grey level co-occurrence matrix (GLCM) to combine the element esteem that is feature level fusion (FLF). The feature vectors classifier is connected to classify the images, here two diverse part works are hybridised in SVM process, that is linear and quadratic kernel function that is MKSVM. The objective output is to distinguish whether the electrical equipment are working under normal or abnormal thermal condition. The motivation behind SVM is to discover a hyperplane that is the

maximal division between the decision function values from two classes. Lastly, the methodologies examined the thermal profiles of all the classified images. Also, the proposed strategy accomplishes better performance contrasted with existing procedures. This entire model appears in Figure 1. This section discussed the four modules such as:

- 1 pre-processing
- 2 segmentation
- 3 feature extraction and FLF
- 4 classification.

**Figure 1** Block diagram for proposed model (see online version for colours)



### 3.1 Pre-processing module

The histogram equalisation periodically offers to ascend to the worldwide differentiation of a few images, particularly when the functional data of the image are symbolised by close complexity values. The histogram equalisation achieves this assignment proficiently by spreading out the most successful power esteems, this formula appeared in equation (1).

$$H_e(i) = \text{round} \left( \frac{cdf(i) - cdf_{\min}}{(W * H) - cdf_{\min}} X (G_i - 1) \right) \tag{1}$$

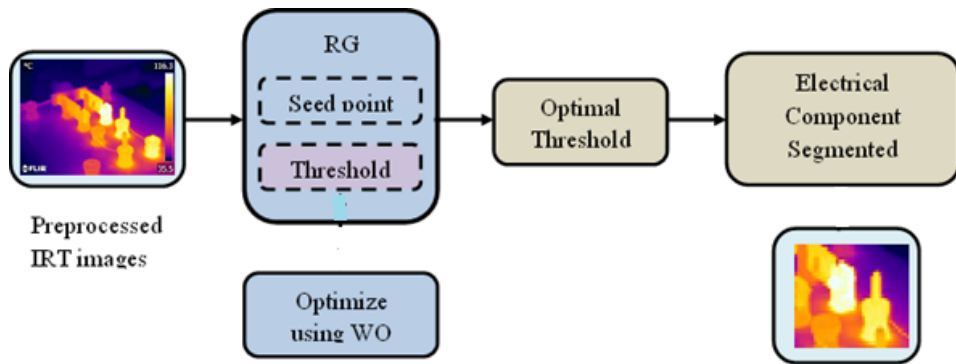
where  $H_e(i)$  is Value of histogram,  $cdf$  is a Cumulative distributive function,  $cdf_{\min}$  is minimum non-zero value of  $cdf$ ,  $G_i$  is Number of grey levels,  $W$  is Width of the Image,  $H$  is Height of the Image.

### 3.2 Segmentation using ORG

In this section, it is effectively segmented the electrical parts like a switch, fuse, connectors utilising the powerful RG strategy with the optimal way that is ORG. Incidentally, the image segmentation speaks to the errand of isolating an advanced image into different segments that are a gathering of pixels in view of guaranteed likeness benchmark, for example, the colour, intensity or texture, with an eye on putting and finding articles and limits in an image.

In the typical RG system, when the intensity imperative is investigated by the neighbouring pixels, some disadvantage emerges in the ordinary RG technique as the shading in the genuine images can't be recognised and furthermore, the possibility of noise to happen in the intensity esteem may bring about finished segmentation. The optimal threshold esteem is anticipated for the better segmentation and this will expand the accuracy of the segmented image optimisation procedures that are used. For optimal threshold process, WO is utilised to enhance the accuracy subsequently involving four stages, appeared in Figure 2 (Gao et al., 2011; Kaveh and Ilchi Ghazaan, 2017).

Figure 2 Workflow of segmentation module (see online version for colours)



#### 3.2.1 Gridding

At initial, the image is separated into various blocks ( $B_n$ ) and as it looks like applying a lattice on the image. The gridding is done to apportion each spot with singular compartments.

#### 3.2.2 Seed point selection

In this procedure, the histogram assessment is utilised to introduce the seed point. In the perspective of the way that the histogram system is utilised for each pixel in the block, the estimation of the pixel lies in the vicinity of 0 and 255 and the most every now and again happening pixel esteem is distributed to be the seed point. On account of every last image, the places are isolated and the seed point is settled.

$$block(i, j) = f_i(u : (u + B_n) - 1, p : (p + B_n) - 1) \text{ for } i = 1, 2, \dots, 10; j = 1, 2, \dots, 10 \quad (2)$$

### 3.2.3 Finding optimal threshold value

This procedure is done to achieve the segmented image and for the reason, the optimisation strategy is linked. In the edge optimisation, the most extreme accuracy is gotten in the WO.

#### Steps for whale optimisation

##### Step 1 Initialisation

Here, the weight value speaks to the random esteem  $r_i (i = 1, 2, \dots, n)$  where  $n$  demonstrates the quantity of weight esteem. And furthermore, instate the coefficient vectors of a whale.

##### Step 2 Fitness evaluation

In each block of the image, it is to find the fitness, in a segmented part and which is the most extreme accuracy of the segmented part.

$$F_i = \max \left( \frac{TP + TN}{TP + TN + FP + FN} \right) \quad (3)$$

where  $TP$  is true positive,  $TN$  is true negative,  $FP$  is false positive and  $FN$  false negative.

##### Step 3 Updating process: encircling prey

Humpback whale surrounds the prey (little fishes) at that point refreshes its position towards the ideal arrangement throughout expanding number of iterations from beginning to the greatest number of iterations. The refreshed strategy is spoken to by the accompanying conditions:

$$\bar{P} = \left| \bar{k} \bar{T}^{best}(t) - \bar{T}(t) \right| \quad (4)$$

$$\bar{T}(t+1) = \bar{T}^{best}(t) - \bar{P} \bar{k}1 \quad (5)$$

where  $\bar{k}$ ,  $\bar{k}1$ ,  $\bar{P}$  are Coefficient Vector,  $t$  is current iteration,  $\bar{T}^{best}(t)$  is position vector of Optimum solution and  $\bar{T}(t)$  is position vector.

The vectors  $\bar{k}1$  and  $\bar{k}$  are calculated using (6) and (7)

$$\bar{k}1 = 2\bar{k}2\bar{r} - \bar{k}2 \quad (6)$$

$$\bar{k} = 2\bar{r}3 \quad (7)$$

where  $\bar{k}2$  is linearly decreased from 2 to 0 over the course of iterations,  $\bar{r}$ ,  $\bar{r}3$  are random vectors in the range (0, 1).

##### Step 4 Exploitation phase: bubble-net attacking method

Keeping in mind the end goal to numerically show the bubble net behaviour of humpback whales, two enhanced methodologies are planned:

a Shrinking encircling mechanism

This process employed by decreasing linearly the value of  $\overline{k2}$  from 0 to 2, the Random value of vector  $\overline{k1}$  range between (-1 to 1).

b Spiral updating position

A spiral condition is then made between the position of whale and prey to copy the helix-formed development of humpback whales as takes after.

$$\overline{T}(t+1) = \overline{P}e^{bt} \cos(2\pi s) + \overline{T}^{best}(t) \tag{8}$$

$$\overline{T}(t+1) = \begin{cases} \overline{T}^{best}(t) - \overline{k1}\overline{P} & \text{if } i < 0.5 \\ \overline{P}e^{bt} \cos(2\pi s) + \overline{T}^{best}(t) & \text{if } i > 0.5 \end{cases} \tag{9}$$

where  $s$  is random value between -1 to +1,  $b$  is constant and  $i$  is between 0 and 1.

To show this synchronous behaviour, it is expected that there is a probability of half to pick between both the contracting encompassing system and the spiral model to refresh the position of whales amid optimisation.

c Search for prey (exploration phases)

A similar approach in view of the variety of the  $\overline{k1}$  vector can be used to look for prey (investigation). Indeed, humpback whales look haphazardly as indicated by the position of each other.

$$\overline{P} = \left| \overline{k} \cdot \overline{T}_{rand} - \overline{T} \right| \tag{10}$$

$$\overline{T}(t+1) = \overline{T}_{rand} - \overline{k1} \cdot \overline{P} \tag{11}$$

This mechanism and  $|\overline{k1}| > 1$  emphasise exploration and allow the WO algorithm to perform a global optimum and  $|\overline{k1}| < 1$  for updating the position of the search agents.

Step 5 Termination criteria

Rehash process, until the point that a superior fitness or most extreme number of iterations is met. In view of the above technique, the ideal threshold is selected in RG and afterward, these ideal thresholds are gone before for additional ventures in RG.

3.2.4 Applying RG to the seed point

The last method is the RG technique, wherein the esteem that is accomplished from the ideal threshold calculation strategy prompts a precise coerced electrical section of the image.

3.3 Feature extraction module

Feature selection is a critical stride where just powerful features will be chosen. Note that the decisions of input features are relying upon the sort and the objective of electrical



equipment. Some input features are appropriate for certain hardware’s while others are exceptionally sufficiently broad to be utilised for most sorts of electrical equipment’s, consider features, for example, are colour and GLCM features (Thobiani et al., 2017).

a Colour feature

Colour feature is a most normal feature of the image. Colour histograms normally utilise content-based image retrieval. Feature implies attributes of the query. Feature extraction alludes that dimensionality decrease of that protest. Colour feature is separated by colour histogram and colour correlogram.

b Grey level co-occurrence matrix

GLCM, also called the grey level spatial dependence lattice, symbolises a factual strategy of assessing the surface that considers the spatial relationship of pixels. The arrangement of grey level co-happening probabilities (GLCP) is characterised by the authors (Karthikeyan and Rengarajan, 2014; Lloyd et al., 2017). From the GLCP dissected some feature vector esteems appeared in Table 1.

$$GP_{ij} = \frac{F_{ij}}{\sum_{i,j=0}^{L-1} F_{ij}} \tag{12}$$

where  $F_{ij} \rightarrow$  the frequency of occurrences between two grey levels,  $L \rightarrow$  Number of quantised grey levels,  $i$  and  $j \rightarrow$  displacement vector for the specified window size.

**Table 1** GLCM features used for proposed model

Autocorrelation	Sum squares
Contrast	Sum average
Correlation	Sum variance
Cluster prominence	Sum entropy
Cluster shade	Difference of variance
Dissimilarity	Difference of entropy
Energy	Information measure of correlation 1
Entropy	Information measure of correlation 2
Homogeneity	Inverse difference normalised (IDN)
Maximum probability	Inverse difference moment normalised (IDM)

Four first-order features specifically mean, standard deviation, entropy and variance are extricated from the pre-processed image. Textural features are then removed utilising GLCM, to speak to an arrangement of features to decrease the misclassification of glaucomatous images. GLCM delineates how diverse blends of pixel brightness values happen in an image.

3.3.1 Feature selection

High dimensional data could contain a high level of excess data and debase the proficiency of the framework. The best subset of features was instated as the vacant set and at each progression, another feature was included. From that point onward, the

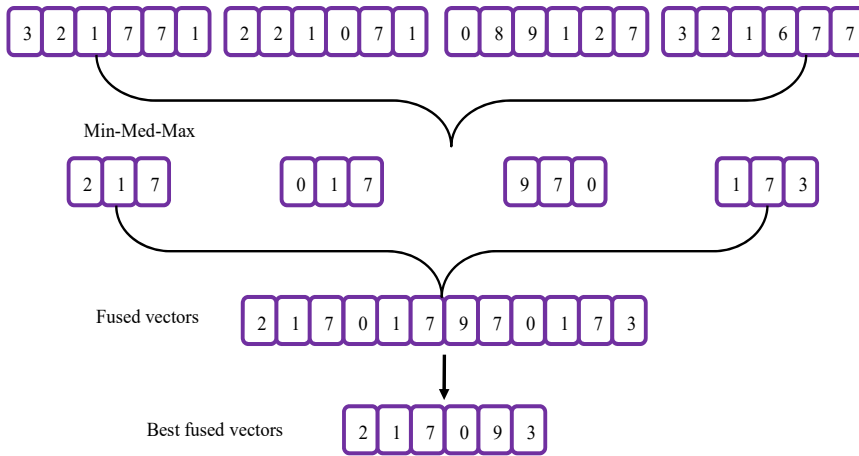
algorithm looks for features that can be evacuated until the point that the right classification error does not increment (Nardi et al., 2016). The ‘best subset’ of features is built in light of the frequency with which each attribute is chosen. The chosen features are given as a contribution to the classification (Huda and Taib, 2013).

### 3.3.2 FLF process

Fundamentally, to fuse information at feature-level is exceptionally extreme or even unimaginable since feature spaces are obscure for various images. This FLF methodology considers the features of two different images. Least and greatest features of images analysed. In FLF as shown up in Figure 3, the feature set starting from segmented image features.

These features are then connected to outline, form a new vector. This normalised fused vector considered for optimisation technique to get ideal feature values. The essential feature standardisation is to modify the range and scale parameters of individual feature qualities to change the incentive into a typical area.

**Figure 3** FLF process (see online version for colours)



### 3.4 IRT image classification module

It is essential to investigate the connection between the seed warm flows distinguished by thermal image and the seed reasonability. Accordingly, feature selection is an imperative stride where just viable features will be chosen. Inconsequential or excess features can add to over-fitting and poor classification exactness. The execution of the particular classifier is utilised to assess the nature of the features. In this IRT image classification module, the MKSVM method is considered. Linear and quadratic kernel functions are the most appropriate kernel function, are to be embraced in this exploration.

#### 3.4.1 SVM model

The SVM approach looks to locate the ideal separating hyperplane between the classes by concentrating on the training cases that are put at the edge of the class descriptors.

These training cases are known as the support vectors. By expanding the base edge between the two sets the relative ideal hyperplane is produced (Zou and Huang, 2015; Lim et al., 2014).

### 3.4.1.1 Multi kernels in SVM

The classification strategy of multi kernel SVM is proposed in our paper. It uses the kernel function to group the data without the utilisation of hyperplanes. The kernel functions for the most part utilised as a part of the training are direct and quadratic articulations.

$$MK = Linear_K(IK, t) + quad_K(IK, t) \quad (13)$$

#### 1 Linear kernel function

The two classes are straightly detachable, which implies that it is attainable to situate not less than one hyperplane characterised by a vector with a bias, which is skilful to isolate the classes with zero error. The linear kernel function is spoken to as takes after.

$$Linear_K(IK, t) = IK^T t + C \quad (14)$$

where  $IK, t \rightarrow$  inner products in linear kernel,  $C \rightarrow$  constant

#### 2 Quadratic kernel function

The quadratic kernel utility in SVM movement is its outcomes in a kernel lattice through the entire rank and thus structure an unbounded estimation attribute break. This is correspondent to handle nonlinear disintegration in the imaginative input break.

$$Quad_K(IK, t) = 1 - \frac{\|IK - t\|^2}{\|IK - t\|^2 + C} \quad (15)$$

Executing a two-dimensional quadratic kernel utility designate the SVM algorithm to find support vectors and suitably split the area.

### 3.4.2 Training phase

The output of feature selection is outfitted as the contribution of the training stage. The information function outfits the arrangement of qualities which cannot be isolated. All the potential isolations of the point set are acknowledged by methods for a hyper plane. However, for characterising vast datasets, it is hard to discover the detachment hyper plane.

### 3.4.3 Testing phase

Testing a model implies that the model is connected to data which as of now contains the objective field values that the model can predict. The test set is utilised for free testing on the system execution. Here we tested six test image and classifier to classify the IRT image as faulted or non-faulted image. This execution of the model created from the

training procedure can be measured by its mean squared error (MSE) value also from percentage error esteem.

### 3.5 Thermal profile analysis of equipment

The presentations for different input features are inspected subsequent to finding the optimal arrangement and the parameters of the classifiers. From the exploratory outcome, the most appropriate input features are the mix of maximum temperature, normal region's temperature and temperature distinction between the objective and reference area. Equipment is analysed with the above data.

## 4 Results and discussions

The consequences of classification and segmentation IRT image are examined with the proposed and existing method with different execution measures like sensitivity, specificity and accuracy. The basic control is to be made for each recognised area. The data are separated into two sets, i.e., training set (80%) and testing set (20%).

### 4.1 Experimental setup

In this area, we exchange the outcome acquired from the proposed system for IRT image segmentation and classification models. This proposed show executed on a windows machine having a course of action Intel processor®, RAM: 4 GB, Speed: 2.50 GHz and the operating system is Microsoft Windows10.

### 4.2 Evaluation parameters

To evaluate the segmentation and classification results, it is considered the true positive (TP) and true negative (TN) as effectively predicted abnormal (fault) and normal (no fault). Conversely, false positive (FP) and false negative (FN) are characterised as false predicted abnormal as well as false predicted normal equipment. And the following parameters are calculated to investigate the segmentation result.

$$\text{Sensitivity} = \frac{TP}{TP + FN}$$

$$\text{Specificity} = \frac{TN}{TN + FP}$$

$$\text{Accuracy} = \frac{TP + TN}{TP + FP + TN + FN}$$

$$\text{Precision (or) PPV} = \frac{TP}{TP + FP}$$

$$\text{Negative predictive value (NPV)} = \frac{TN}{TN + FN}$$

$$\text{False predictive value (FPR)} = \frac{FP}{FP + TN}$$

$$\text{False discovery rate (FDR)} = \frac{FP}{TP + FP}$$

$$\text{False negative rate (FNR)} = \frac{FN}{TP + FN}$$

$$\text{Random index (RI)} = \frac{l + m}{l + m + n + o}$$

where  $l + m$  is the number of agreements between the partitions  $A$  and  $B$  and  $n + o$  is the number of disagreements between the partitions  $A$  and  $B$ .

$$\text{Global consistency error(GCE)} = \frac{1}{n} \min \left\{ \sum_i E(S_1.S_2, p_i), \sum_i E(S_2.S_1, p_i) \right\}$$

where two segmentations  $S_1$  and  $S_2$  as input, these values contain pixel

$$\text{Variation of information (VI)} : VI(A, B) = H(A) + H(B) - 2I(A, B)$$

where  $H(A)$  is entropy of  $A$  and  $I(A, B)$  is mutual information between  $A$  and  $B$ .

### 4.3 Database description

Thermal imager was used to capture the image of electrical equipment. Here, 200 images are considered. From that 600 areas were effectively recognised and all the related features were extracted.

The classification and segmentation performances can be assessed in a few ways. The most usually utilised techniques for classification quality are worked from a perplexity grid, which records accurate and inaccurate acknowledgment.




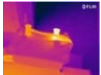








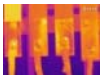


**Figure 4** Sample database images (see online version for colours)



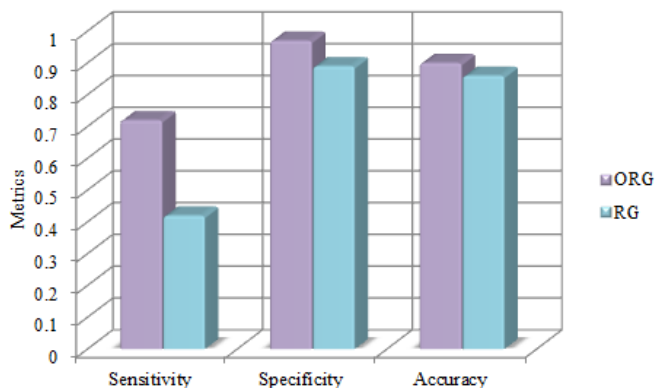
4.4 Results of segmentation analysis

Table 1 demonstrates the IRT thermal images with segmentation part and execution measurements of ORG and RG. Maximum execution accuracy, sensitivity and specificity achieved the values as 95.36%, 86.11% and 97.99% in ORG and 49.84, 29.85 and 99.56 respectively in the RG segmentation system analysis. Possible to watch that the maximum temperature is not changed by the optimisation. Just the base and mean temperatures of the dissected images are impacted. RG technique offers the most noticeably bad segmentation results where the image is said to be over-divided. Optimal thresholding strategy has demonstrated a noteworthy change in contrast with the past segmentation, utilising unique infrared image. Figures 5(a), 5(b) and 5(c) are exploring the distinction execution and the accuracy of the segmentation strategies are assessed based on parameters of false discovery rate (FDR), false positive rate (FPR) and global consistency error (GCE). Through an examination of every single tested image utilising RG strategies, the segmentation accuracy is not surpassed over 10%, even in the wake of applying the proposed image improvement system. Adding up to the execution of all parameter measurements better values in RG-WO model. Table 2 clearly shows that elements min, med and max feature values beat over other input features which yield 98.56% as far as sensitivity, specificity, accuracy and precision. The most important classification performance is accomplished when the parameter estimation of 99.2% in precision correspondingly.

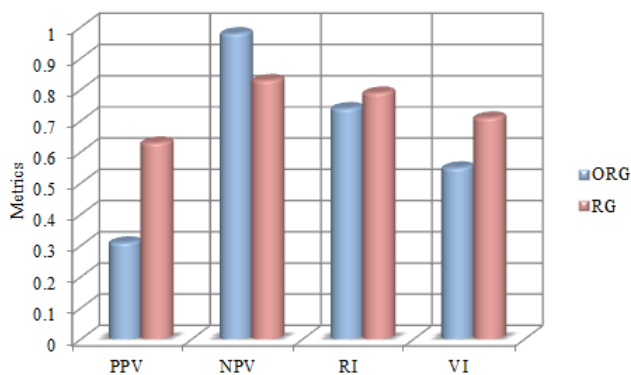
**Table 1** Performance measure for proposed and existing model (see online version for colours)

Input image	Segmented part		Accuracy (%)		Sensitivity (%)		Specificity (%)	
	ORG	RG	ORG	RG	ORG	RG	ORG	RG
			95.36	49.84	86.11	29.85	97.99	99.56
			91.04	86.5	100	41.4	90.88	95.13
			81.56	90.16	90.01	80.45	78.28	99.79
			89.07	87.45	99.65	78.9	85.44	97.5
			61.74	81.17	12.35	66.74	62.56	98.356

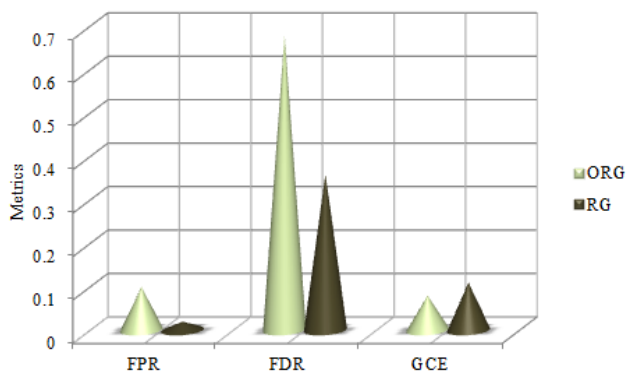
**Figure 5** (a) Comparison of sensitivity, specificity and accuracy of ORG and RG (b) Comparison of PPV, NPV, RI and VI of ORG and RG (c) Performance metrics analysis for segmentation (see online version for colours)



(a)



(b)



(c)

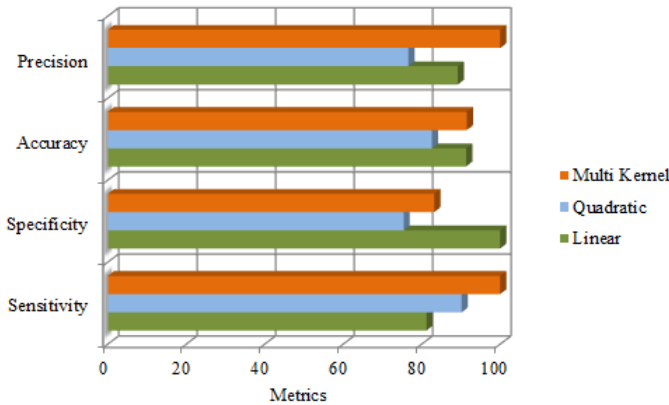
**Table 2** Feature vector min-max values and classification model (MK SVM)

Images	Feature vector			Accuracy	Sensitivity	Specificity	Precision
	Min	Med	Max				
1	-0.618	2608.3	119.75	90.2	100	90.5	78.5
2	-0.79	1720.3	75.54	91.2	72.5	84.56	84.56
3	-0.641	504.29	23.9	100	75.4	85.26	88.4
4	-0.681	494.86	24.51	85.6	82.2	82.2	81.2
5	-0.832	97	6.478	81.2	83.3	85.6	88.2

#### 4.5 Classification results

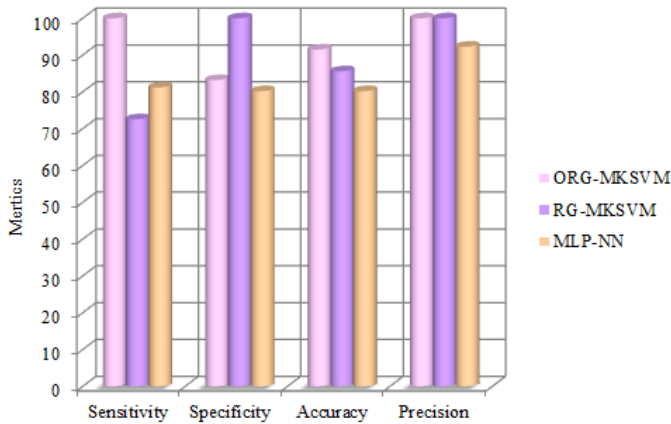
Figure 6 demonstrates the classification execution significances of the linear, quadratic and multi-kernel function. Classifiers at the training stage are connected in the testing stage. The feature is chosen as the input for the three types of classifiers. It demonstrates that MK SVM classifier is marginally superior to SVM in all perspectives aside from specificity. The general accuracy of this classifier is around 99.026% near the perfect which shows a decent performance. It is clearly can be reasoned that component is beaten over other input features which yield 100% as far as sensitivity, specificity, precision and accuracy. Figure 7 explores the comparative analysis of sensitivity, specificity, accuracy and precision of various systems. In comparison, the optimal parameters attained for MLP and SVM classifiers at the training stage are connected in the testing stage. As for all executed files for different input features, it is concluded that the ORG-MK SVM feature set is the best determination for identifying the thermal fault in electrical establishments. While the decision of classifier between the MLP and SVM has a very little noteworthy impact to the classification execution.

**Figure 6** Classification performance results (see online version for colours)

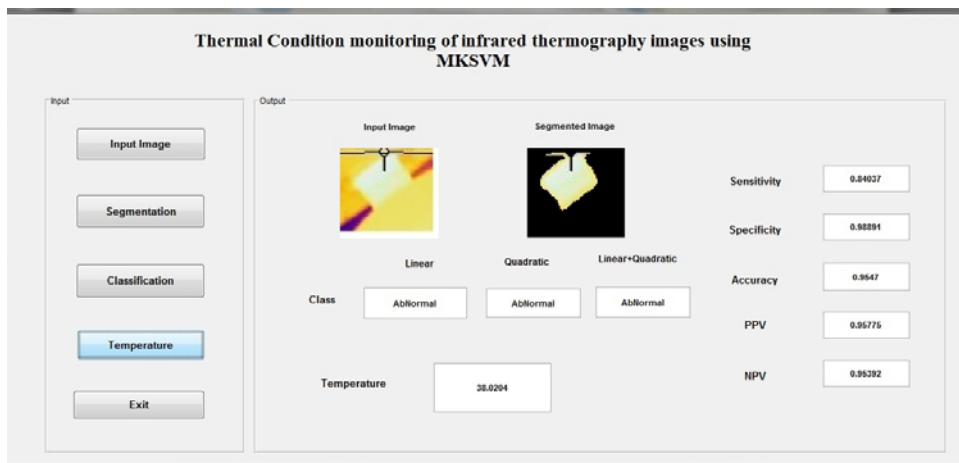




**Figure 7** Comparative feature set analysis of different classification models (see online version for colours)



**Figure 8** GUI for proposed model (see online version for colours)



To guarantee that a continuous power supply which is input to the electrical part, the reliability of the electrical power apparatus must be verified consistently for the ordinary operation of the machine or any segment of a machine. A maximum temperature of 70°C is quite high for an electrical part, however, it is substantially more disturbing if the encompassing temperature is 20°C than if the encompassing temperature is 50°C. Figure 8 demonstrates the principal window of the user interface (UI) program. The framework will naturally assess the coupling of the DC generator condition when the diagnosis button is clicked and the outcome will show up immediately. Subsequent to choosing the objective locales inside the image, the software will process the image and the outcome will show up in the wake of pressing the button. Here, the compulsory limitations with the input on the premise of various techniques execution parameters are surveyed. In this graphical user interface (GUI) based technique, the input values are restored and the acclimating outputs are examined.

## 5 Conclusions

This paper discussed the IRT image segmentation, classification systems with temperature examination. The technique for finding reasonable input features for distinguishing the thermal fault in electrical establishments is exhibited. Segmentation process accomplishes better execution in RG with threshold optimisation process and for classification, quadratic kernel function utilised. Utilising a wrapper show approach for feature selection, the classification exhibitions for different input features are inspected in the wake of finding the optimal design and parameters of the classifiers. From the investigation result, the most reasonable input features are the blend of maximum temperature, normal region's temperature and temperature contrast between the objective and reference location. This proposed scheme attained the maximum accuracy at 98.62% with MKSVM classifier. The results can be improved by using, optimal feed forward back propagation neural network (FFBN) to distinguish IRT faulted equipment image with temperature values.

## References

- Ahmed, M.M., Huda, A.S.N. and Isa, N.A.M. (2015) 'Recursive construction of output-context fuzzy systems for the condition monitoring of electrical hotspots based on infrared thermography', *Journal of Engineering Applications of Artificial Intelligence*, Vol. 39, pp.120–131.
- Almeida, C.A.L., Braga, A.P., Nascimento, S., Paiva, V. and Martins, H.J.A. (2009) 'Intelligent thermographic diagnostic applied to surge arresters: a new approach', *Power Delivery*, Vol. 24, No. 2, pp.751–757.
- Chouder, A. and Silvestre, S. (2010) 'Automatic supervision and fault detection of PV systems based on power losses analysis', *Energy Conversion and Management*, Vol. 51, No. 10, pp.1929–1937.
- Coleman, A. and Zalewski, J. (2011) 'Intelligent fault detection and diagnostics in solar plants', *IEEE 6th International Conference on Intelligent Data Acquisition and Advanced Computing Systems (IDAACS)*, pp.948–953.
- Ducange, P., Fazzolari, M., Lazzarini, B. and Marcelloni, F. (2011) 'An intelligent system for detecting faults in photovoltaic fields', *11th International Conference on Intelligent Systems Design and Applications (ISDA)*, pp.1341–1346.
- Gao, Y., Mas, J.F., Kerle, N. and Pacheco, J.A.N. (2011) 'Optimal region growing segmentation and its effect on classification accuracy', *International Journal of Remote Sensing*, Vol. 32, No. 13, pp.3747–3763.
- Haddadnia, A.R.J. and Seryasat, O. (2010) 'Intelligent fault detection of electrical equipment in ground substations using thermo vision technique', in *Proceeding of the 2nd International Conference on Mechanical and Electronics Engineering (ICMEE)*, Vol. 2, pp.150–154.
- Huda, A.S.N. and Taib, S. (2013) 'Suitable features selection for monitoring thermal condition of electrical equipment using infrared thermography', *Journal of Infrared Physics and Technology*, Vol. 61, pp.184–191.
- Huda, A.S.N., Taib, S., Ghazali, K.H. and Jadin, M.S. (2014) 'A new thermographic NDT for condition monitoring of electrical components using ANN with confidence level analysis', *ISA Trans.*, Vol. 53, No. 3, pp.717–724.
- Huda, A.S.N., Taib, S., Jadin, M.S. and Ishak, D.A. (2012) 'Semi-automatic approach for thermographic inspection of electrical installations within buildings', *Energy Build*, Vol. 55, pp.585–591.

- Jadin, M.S., Taib, S. and Ghazali, K.H. (2014) 'Feature extraction and classification for detecting the thermal faults in electrical installations', *Journal of Measurement*, Vol. 57, pp.15–24.
- Jaffery, Z.A. and Dubey, A.K. (2014) 'Design of early fault detection technique for electrical assets using infrared thermograms', *Int. J. Electr. Power Energy Syst.*, Vol. 63, pp.753–759.
- Karthikeyan, S. and Rengarajan, N. (2014) 'Performance analysis of gray level co-occurrence matrix texture features for glaucoma diagnosis', *American Journal of Applied Sciences*, Vol. 11, No. 2, pp.248–257.
- Kaveh, A. and Ilchi Ghazaan, M. (2017) 'Enhanced whale optimization algorithm for sizing optimization of skeletal structures', *Mechanics Based Design of Structures and Machines*, Vol. 45, No. 3.
- Lim, G-M., Bae, D-M. and Kim, J-H. (2014) 'Fault diagnosis of rotating machine by thermography method on support vector machine', *Journal of Mechanical Science and Technology*, Vol. 28, No. 8, pp.2947–2952.
- Lloyd, K., Rosin, P.L., Marshall, D. and Moore, S.C. (2017) 'Detecting violent and abnormal crowd activity using temporal analysis of grey level co-occurrence matrix (GLCM)-based texture measures', *Machine Vision and Applications*, Vol. 28, No. 8, p.361–371.
- Nardi, I., Paoletti, D., Ambrosini, D., de Rubeis, T. and Sfarra, S. (2016) 'U-value assessment by infrared thermography: a comparison of different calculation methods in a guarded hot box', *Journal of Energy and Buildings*, Vol. 122, pp.211–221.
- Pratama, M., Anavatti, S. and Lu, J. (2015) 'Recurrent classifier based on an incremental meta-cognitive-based scaffolding algorithm', *IEEE Transactions on Fuzzy Systems*, Vol. 23, No. 6, pp.2048–2066.
- Pratama, M., Angelov, P., Lughofer, E. and Er, M-J. (2018b) 'Parsimonious random vector functional link network', *Information Sciences*, Vols. 430–431, pp.519–537.
- Pratama, M., Lu, J. and Zhang, G. (2016) 'Evolving type-2 fuzzy classifier', *IEEE Transactions on Fuzzy Systems*, Vol. 24, No. 3, pp.574–589.
- Pratama, M., Pedrycz, W. and Lughofer, E. (2018a) 'Evolving ensemble fuzzy classifier', *IEEE Transactions on Fuzzy Systems*, DOI: 10.1109/TFUZZ.2018.2796099.
- Riley, D. and Johnson, J. (2012) 'Photovoltaic prognostics and heat management using learning algorithms', *38th Conference (PVSC), IEEE*, pp.001535–001539.
- Stoicescu, L., Reuter, M. and Werner, J.H. (2014) 'Luminescence imaging of PV modules in daylight', *European Photovoltaic Solar Energy Conference and Exhibition (Eu Pvsec)*, Amsterdam, Netherlands.
- Sujatha, K. and Shalini Punithavathani, D. (2018) 'Optimized ensemble decision-based multi-focus image fusion using binary genetic Grey-Wolf optimizer in camera sensor networks', *Multimedia Tools and Applications*, January, Vol. 77, No. 2, pp1735–1759.
- Sundararaj, V. (2016) 'An efficient threshold prediction scheme for wavelet based ECG signal noise reduction using variable step size firefly algorithm', *Int. J. Intell. Eng. Syst.*, Vol. 9, No. 3, pp.117–126.
- Takashima, T., Yamaguchi, J., Otani, K., Oozeki, T., Kato, K. and Ishida, M. (2009) 'Experimental studies of fault location in PV module strings', *Solar Energy Materials and Solar Cells*, Vol. 93, pp.1079–1082.
- Thobiani, F.A., Tran, V.T. and Tinga, T. (2017) 'An approach to fault diagnosis of rotating machinery using the second-order statistical features of thermal images and simplified fuzzy ARTMAP', *Engineering*, Vol. 9, No. 6, pp.524–539.
- Tsanakas, J.A., Chrysostomou, D., Botsaris, P.N. and Gasteratos, A. (2015a) 'Fault diagnosis of photovoltaic modules through image processing and Canny edge detection on field thermographic measurements', *International Journal of Sustainable Energy (T&F)*, Vol. 34, No. 6, pp.351–372.

- Tsanakas, J.A., Vannier, G., Plissonnier, A. and Barrue, I.F. (2015b) 'Fault diagnosis and classification of large-scale photovoltaic plants through aerial ortho-photo thermal mapping', *Proc. of 31st European Photovoltaic Solar Energy Conference and Exhibition (EUPVSEC)*, Hamburg, Germany.
- Zou, H. and Huang, F. (2015) 'A novel intelligent fault diagnosis method for electrical equipment using infrared thermography', *Journal of Infrared Physics and Technology*, Vol. 73, pp.29–35.